

---

# DISCOVER: DEEP IDENTIFICATION OF SYMBOLIC OPEN-FORM PDES VIA ENHANCED REINFORCEMENT-LEARNING

---

**Mengge Du**

College of Engineering  
Peking University  
Beijing  
2101111985@stu.pku.edu.cn

**Yuntian Chen**

Eastern Institute for Advanced Study  
Yongriver Institute of Technology  
Ning bo  
ychen@eias.ac.cn

**Dongxiao Zhang**

National Center for Applied Mathematics Shenzhen (NCAMS)  
Southern University of Science and Technology  
Shen zhen  
zhangdx@sustech.edu.cn

## ABSTRACT

The working mechanisms of complex natural systems tend to abide by concise and profound partial differential equations (PDEs). Methods that directly mine equations from data are called PDE discovery, which reveals consistent physical laws and facilitates our interaction with the natural world. In this paper, an enhanced deep reinforcement-learning framework is proposed to uncover symbolic open-form PDEs with little prior knowledge. Specifically, (1) we first build a symbol library and define that a PDE can be represented as a tree structure. Then, (2) we design a structure-aware recurrent neural network agent by combining structured inputs and monotonic attention to generate the pre-order traversal of PDE expression trees. The expression trees are then split into function terms, and their coefficients can be calculated by the sparse regression method. (3) All of the generated PDE candidates are first filtered by some physical and mathematical constraints, and then evaluated by a meticulously designed reward function considering the fitness to data and the parsimony of the equation. (4) We adopt the risk-seeking policy gradient to iteratively update the agent to improve the best-case performance. The experiment demonstrates that our framework is capable of mining the governing equations of several canonical systems with great efficiency and scalability.

**Keywords** Structure-aware LSTM agent · Deep reinforcement learning · symbolic representation · PDE discovery

## 1 Introduction

Discovering the laws of physics in the natural world is of great significance for us to understand how the world operates. Many physical phenomena in dynamic natural systems can be expressed by concise and elegant nonlinear governing equations. In the past, the mining of these equations was often based on first principles, whose application was very limited, and domain knowledge of experts in the specific field was required. With the development of some intelligent algorithms, such as the genetic algorithm (GA), especially the rise of deep learning, the ability to uncover nonlinear relationships of complex physical systems has been greatly empowered, and time consumption has been markedly reduced.

The essence of mining natural laws in dynamic systems is to find the relationship between the state variables and their derivatives in space and time through observations, so as to extract the governing equations that can satisfy the laws of physics (e.g., conservation laws). Sparse regression is an essential and commonly used method to accomplish the PDE discovery task. SINDy [1] first utilized sparsity-promoting to identify the most important function terms that conform to the data, in order to obtain an accurate and concise equation representation. Then, PDE-FIND [2] further

explored other more complex and high-dimensional dynamic systems, such as the Navier-Stokes equation, using the method of sequential threshold ridge regression (STRidge). Based on SINDy, numerous variants were put forward to improve the sparse regression method, and state-of-the-art (SOTA) performance was achieved [3, 4, 5, 6]. Despite the great success achieved, this series of methods are limited to a fixed and overcomplete candidate library. On the one hand, the selection of candidate functions requires strong prior knowledge. Otherwise, the computational burden will be dramatically increased. On the other hand, although sparse regression can determine the possible function terms and their coefficients simultaneously, it can only generate linear combinations of these candidates, and the expressive ability is highly limited. In order to solve this problem, follow-up research proposed various models and algorithms. PDE-Net [7] utilized learnable filters to numerically approximate differential operators and applied neural networks or other machine learning methods to approximate unknown nonlinear responses, but failed to provide an analytical expression. PDE-Net 2.0 [8] first defined the basic function elements and then generated new interaction terms based on the design of the symbolic neural network which could approximate the nonlinear response. Compared with SINDy, it has a more compact library, and the computational cost is significantly reduced. However, only multiplication and addition operations are introduced in the generation of interactive function terms. It is still deficient in producing the division operation and compound derivatives. DLGA [9] incorporated GA to significantly expand the original candidate set through the recombination of gene fragments (mutation and crossover operations). Nevertheless, the expressive power of the interactive space remains limited, and it is insufficient to discover open-form equations. SGA-PDE [10] further adopted symbolic representations and GA, and represented each function term with a tree structure. Any PDEs can be formulated based on the interaction and combination of different function terms. This method greatly increases representation flexibility, but crossover and mutation operations may lead to poor iterative stability of the generated equation form, which then results in a significant increase in computation time.

In fact, uncovering physical laws through the free combinations of operators and symbols has achieved great progress in symbolic regression due to its great flexibility and little requirements for prior knowledge. In early work, Schmidt et al. discovered analytic relations automatically from experimental data [11]. Bongard et al. introduced an advanced approach by combining partitioning, automated probing, and snipping to facilitate modeling of complex nonlinear dynamics [12]. Later, due to the advantages of the evolutionary methods in solving optimization problems, many symbolic regression algorithms based on GA were put forward [13, 14, 15, 16]. GA enhances exploration ability through some operations on the evolution of individuals (i.e., mathematical expressions), such as crossover and mutation. At the same time, the offspring are screened by the fitness function (e.g., Akaike information criterion) to obtain a better result in the subsequent generation. However, it also causes instability in the iterative process and is more vulnerable to noise. With the progress and development of deep learning, neural networks are gradually being leveraged to reveal common laws in nonlinear dynamic systems. Its application can be divided into two categories. One is to generate a flexible combination of operations and state variables by adjusting the network topology. The representative models are the equation learner (EQL) [17, 18] and its variants in PDE-Net 2.0 [8]. They all belong to supervised learning and optimize the network by minimizing the mean squared error (MSE). The other is based on the idea of reinforcement-learning. The initial mathematical expressions are generated by the agent and only expressions with larger rewards are retained to update the agent, which in turn promotes better expressions. The Monte Carlo tree search based symbolic physics learner (SPL) [19] and the RNN based DSR [20] have both achieved SOTA on many symbolic regression tasks. Moreover, some attempts to combine GA and RL also show great potential to solve real world regression problems [21, 22]. Few studies, however, focus on the PDE discovery task. Symbolic regression focuses on finding a single regression target, and cannot be used to discover governing equations containing abundant physical information (including complex partial differential terms). Due to the focus on fitting the expressions to the measurements, relevant algorithms are liable to suffer from overfitting problems and generate redundant terms.

To ameliorate the limitation of fixed candidate libraries in the past PDE discovery methods and accelerate the search process, we propose a framework, **Deep Identification of Symbolic Open-form PDEs via Enhanced Reinforcement-learning (DISCOVER)**, which can efficiently uncover the concise and meaningful governing equations underlying complex systems. Our contribution mainly lies in the following three aspects:

- We design a novel structure-aware long short-term memory (LSTM) recurrent neural network as the agent that can generate symbolic PDE expressions. It combines structured input and monotonic attention to make full use of historical and structural information, and effectively learn the desired expressions of equations. STRidge is also well combined to determine the coefficients of function terms.
- By means of the domain knowledge of physical and mathematical laws, customized constraints are designed to avoid unreasonable expressions and reduce the search space. A new rewarding function is introduced to ensure parsimony of the discovered equations under the condition that it strictly conforms to observations.
- We demonstrate that our framework can handle the discovery of open-form PDEs according to experiments on multiple canonical dynamic systems, including the Korteweg-de Vries equation, the nonlinear Burgers’

equation (KdV), the Chafee-Infante equation, and PDEs even with fractional structure and compound terms. Its computational efficiency has been significantly improved compared to SGA-PDE.

## 2 Methods

A nonlinear dynamic system can usually be represented by a parameterized PDE given by:

$$u_t = F(u, u_x, u_{xx}, \dots, x, \xi) = \Theta(u, x) \cdot \xi \quad (1)$$

where  $u$  is the observations of interest collected from experiments or nature;  $u_t$  is the first-order time derivative term; and  $F$  is a nonlinear function on the right-hand side, consisting of  $u$  and its space derivatives with different orders (e.g.,  $u_x$  and  $u_{xx}$ ). Taking Burgers' equation as an example,  $F = au_{xx} - buu_x$ . The coefficients of those candidate terms in  $F$  can be represented by  $\xi$ .  $\Theta(u, x)$  is our target with a more concise form.

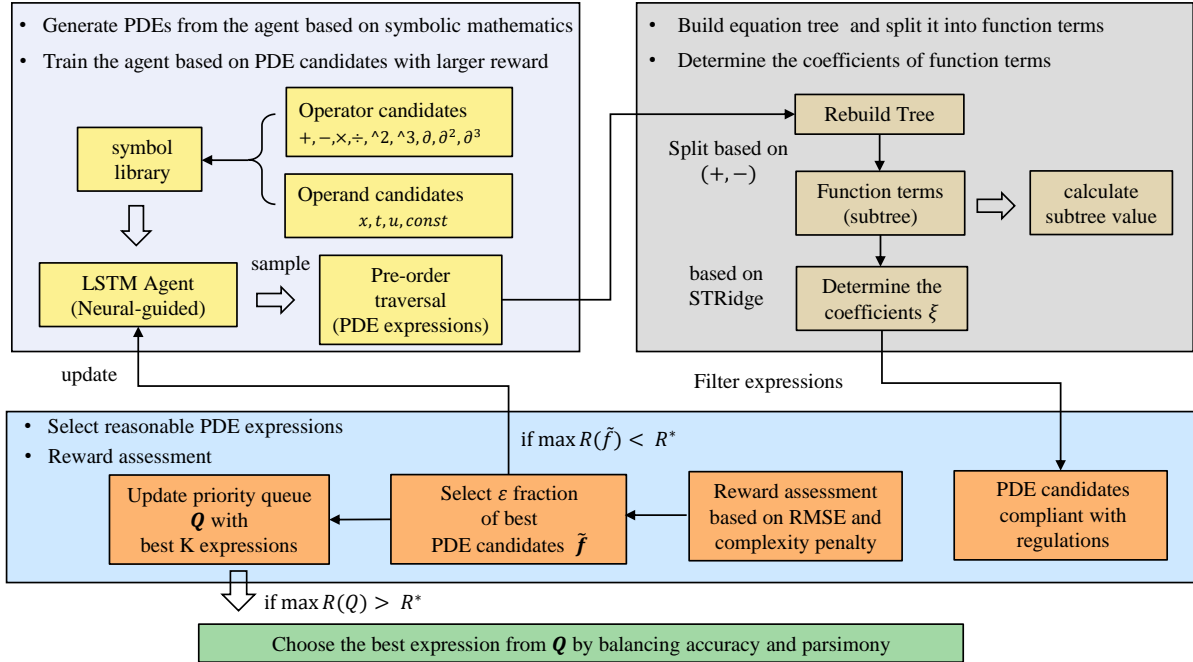


Figure 1: The procedure of DISCOVER framework.  $R^*$  is the predefined reward threshold to terminate the search process and the priority queue  $Q$  is a dynamically updated queue with  $K$  expressions. Whenever there are rewards higher than the internal expressions, the new expressions enter the queue and expressions with lower rewards leave the queue.

The procedure of DISCOVER uncovering PDEs from data are demonstrated in Figure 1, comprising three parts: (1) Generate the pre-order traversals of the PDE expressions based on a predefined symbol library; (2) reconstruct the expression tree and determine the coefficients  $\xi$ ; and (3) select reasonable PDE expressions with higher rewards and iteratively update the agent with the risk-seeking policy gradient method to generate better-fitting expressions.

### 2.1 Generating the pre-order traversals of the PDE expression trees

The basic unit of modeling in SGA is the function term. Each function term can be represented by a binary tree, and the final equation is a forest with a linear combination of all of the function terms. In this problem, we model directly based on the whole equation, i.e., an equation is a tree generated by the agent, and the coefficients of function terms are not included in the tree.

**PDE expression tree.** As shown in Figure 2 (2.a), a PDE expression tree is represented via symbolic representation, and all of the tokens on the nodes are selected from a pre-defined library  $\mathcal{L}$ . The library is shown in Figure 2 (1.a),

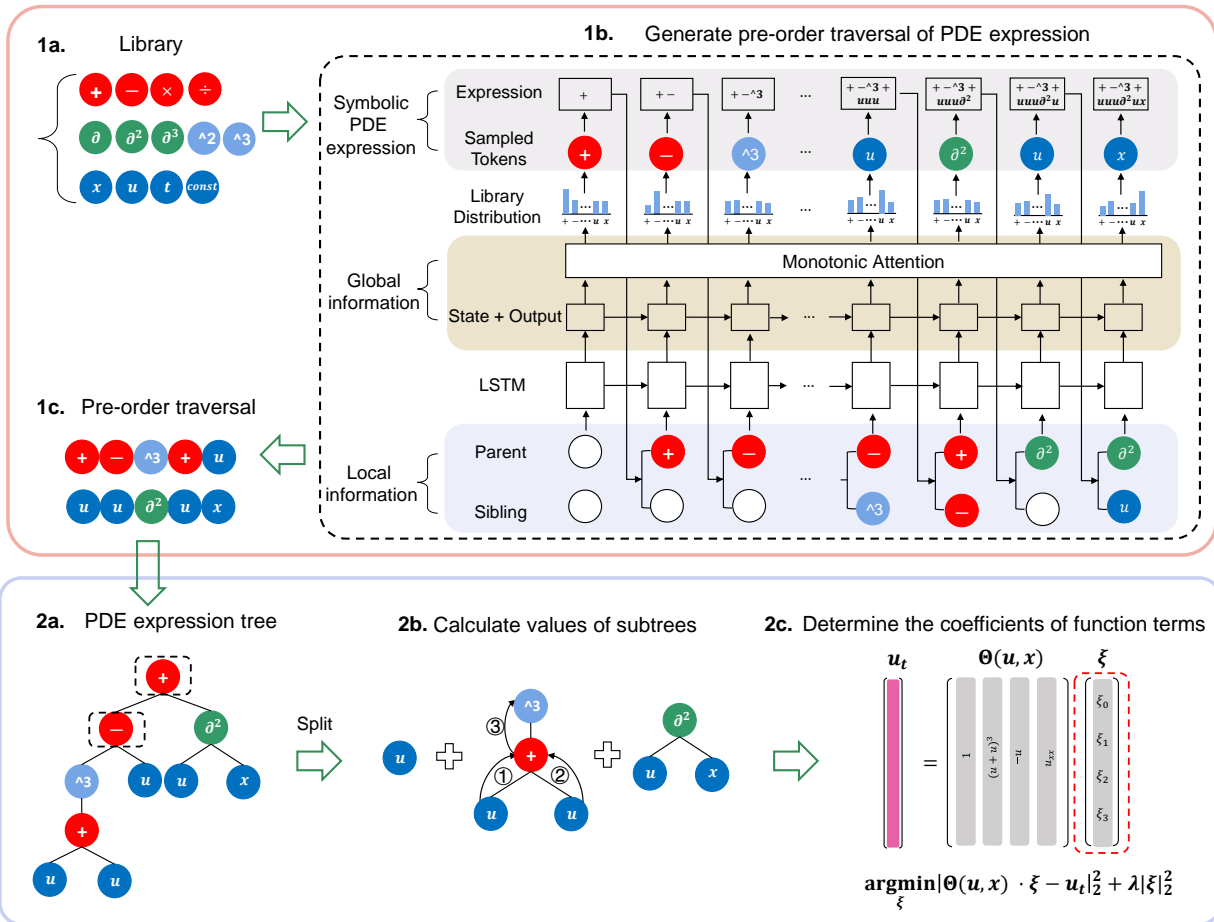


Figure 2: Example of generating a possible expression solution  $u_t = u_{xx} - u + 0.1250(u + u)^3$  for the Chafee-Infante equation. **(1.a)** The pre-defined library consists of all of the operators and operands to generate the open-form PDEs. **(1.b)** The process of generating the pre-order traversal of the expression tree from the structure-aware LSTM agent. The output of the LSTM at each time-step is the probability distribution of all tokens in the library, and then one of the tokens is sampled based on it. The inputs of LSTM are the parent node and sibling node of the current token in the corresponding expression tree. The non-existent nodes are represented by empty circles. The agent combines local information from structured inputs and global information obtained from attention. **(1.c)** The final pre-order traversal of the expression tree. **(2.a)** The PDE expression tree is reconstructed from the corresponding pre-order traversal. **(2.b)** Split the expression tree into subtrees according to the plus and minus operators at the top of the tree, and traverse to calculate each term's value. **(2.c)** Calculate the coefficients of the function terms based on STRidge.

including two categories of symbols: operators (the first two rows) and operands (the bottom row). Compared with the symbolic regression problem, our library also introduces a differential operator with different orders to calculate the time and space derivatives of state variables.

Note that for a PDE expression tree, the interior nodes are all operators, the leaf nodes are all operands, and their arities are known. For example, the partial derivative  $\partial$  is a binary operator with two children and the space input  $x$  is a operands with zero children. This property ensures that each expression tree has a unique pre-order traversal sequence corresponding to it. As a consequence, we can conveniently generate batches of pre-order traversal sequences by means of the LSTM agent instead of the expression trees. An expression tree and its pre-order traversal can be represented as  $\tau$ . The  $i$ -th token in the traversal can be represented as  $\tau_i$  and corresponds to an action under the current policy in reinforcement-learning. When generating the token at the current time-step, the output of LSTM will be normalized to generate a probability distribution of all tokens in  $\mathcal{L}$ . The current action is then sampled based on this distribution. A full binary tree is constructed when all leaf nodes in the expression tree are operands, and the generation process is terminated.

**Structure-aware LSTM agent.** The common LSTM is an autoregressive model, which means that predicting current token  $\tau_i$  is conditioned on the last predicted token  $\tau_{i-1}$ . Because all of the history information is coupled and stored in a cell, it is insufficient for LSTM to deal with long sequences and structural information. To effectively generate the PDE expression trees that have strong structural information, we propose a structure-aware architecture for the LSTM agent. Specifically, (1) learning from DSR [20], we use structured input to convey local information. For example, for the seventh token  $u$  in Figure 2 (1.c), the inputs are its parent (+) and sibling ( $\wedge^3$ ), instead of the previous token  $u$ . (2) The monotonic attention is leveraged to endow the agent with a more powerful capacity to capture global dependencies, and avoids the loss of long-distance information in the step-by-step transmission process. The details of the monotonic attention layer are provided in Appendix A.

**Constraints and regulations.** Generating PDE expression sequences in an autoregressive manner without restrictions tends to produce unreasonable samples. To reduce the search space and time consumption, we design certain constraints based on mathematical rules and physical laws: (1) the minimum and maximum number of the sum of the plus and minus operators are pre-set to control the number of function terms and sequence length; (2) the right child node of partial differential operators (e.g.,  $\partial$ ) must be space variables (e.g.,  $x$ ); (3) the left child node of  $\partial$  cannot be space variables; and (4) the plus and minus operator cannot appear in the descendants of  $\partial$  (optional). In the specific implementation process, these constraints are applied prior to the sampling process, and the probability of the tokens that violate constraints is set to zero. Applying these constraints is convenient and extensible, and can also be incorporated with other domain knowledge. In addition to restricting the generated equations in the generation period, we also establish a series of regulations to double-check the generated equations to withdraw the illegal expressions, such as no state variables included.

## 2.2 Determine coefficients of the PDE expression

**Reconstruct and split the expression tree.** After obtaining the pre-order traversal sequence of PDE, we first need to reconstruct it into the corresponding tree structure. Then, we can split it into subtrees, i.e., the function terms, based on the plus and minus operators at the top of the expression tree, as illustrated in Figure 2 (2.a and 2.b). Subsequently, we solve for the value of each function term over the whole spatiotemporal domain. In the specific solution process,  $(u + u)^3$  in Figure 2 (2b) is taken as an instance. We traverse the subtree from bottom to top in a post-order traversal manner (①->②->③), and then perform operations at each parent node (operators). At this time, the values of its corresponding child nodes have already been calculated.

**STRidge.** STRidge is a widely used method in sparse regression, which can effectively determine non-trivial function terms and find a concise equation by using the linear fit to observations. As shown in Figure 1 (2.c), it can be utilized to solve for the coefficients of each function term based on the results in the previous step. Note that 1 is incorporated as a default constant term.

$$\xi = \arg \min_{\xi} |\Theta(u, x) \cdot \xi - u_t|_2^2 + \lambda |\xi|_2^2 \quad (2)$$

where  $\lambda$  measures the importance of the regularization term. In order to prevent overfitting, we also set a threshold  $tol$ , and function terms with coefficients less than  $tol$  will be directly ignored. More details can be found in PDE-FIND [2].

### 2.3 Training the agent with the risk-seeking policy gradient method

**Reward function.** In order to effectively evaluate the generated PDE candidates, we design a reward function for the PDE discovery problem that comprehensively considers the fitness of observations and the parsimony of the equation. Assuming that the generated PDE expression is  $g$ , it is formulated as follows:

$$R = \frac{1 - \zeta * n}{1 + RMSE}, \quad RMSE = \sqrt{\frac{1}{N} \sum_{i=1}^N (u_{t_i} - g(u, x))^2} \quad (3)$$

where  $n$  is the number of function terms of the governing equation;  $\zeta$  is the penalty factor for parsimony, which is generally set to a small number without fine-tuning, such as 0.01; and  $N$  denotes the number of observations. It can be seen that the root mean squared error (RMSE) in the denominator evaluates the fitness of the PDE candidates to the data. The nominator is an evaluation of the parsimony, thus avoiding overfitting caused by redundant terms.

**Risk-seeking policy gradient method.** Different from PDE-Net 2.0 [8], in this problem, we cannot directly establish the computational graph between rewards and generated expression trees, and utilize gradient descent to update the model parameterized by  $\theta$ . Therefore, we adopt the deep reinforcement-learning training strategy. Specifically, the generated PDE expression sequences are equivalent to the episodes in RL, and the generation process of each token corresponds to the selection of actions. It is worth noting that the total reward is not the sum of each action with a discount factor, but rather is based on the evaluation of the final sequence. The policy  $\pi_\theta$  refers to the distribution over the PDE expression sequences  $p(\tau|\theta)$ . The standard policy gradient is a risk-neural method, i.e., its goal is to maximize the expectation of the generated policy, and the return is as follows:

$$J(\pi_\theta) = \mathbb{E}_{\tau \sim P^{\pi_\theta}} [R(\tau)] \quad (4)$$

However, for problems like PDE discovery, our intention is to ensure that the best-case sample is adequate for the problems, similar to symbolic regression [23, 24] and neural architecture search (NAS) [25]. By referring to the method of risk-seeking policy gradient in DSR [20], we train agents to improve the best-case performance, instead of the average performance, to alleviate the mismatch between the objective and performance evaluation. The idea of this method comes from a well-known risk measure, conditional value at risk (CVaR), defined as  $CVaR_\varepsilon(R) = \mathbb{E}[R | R \leq q_\varepsilon(R)]$ , where  $q_\varepsilon$  is the  $\varepsilon$  quantile of the rewards. It is designed to improve the worst samples in the current policy and avoid risks, and is usually applied in vehicle driving or finance[26, 27, 28]. In contrast, the optimization objective of risk-seeking is the expectation of the  $(1 - \varepsilon)$ -quantile of the rewards  $\tilde{q}_\varepsilon(R)$ . Its return is given by:

$$J_{\text{risk}}(\theta; \varepsilon) \doteq \mathbb{E}_{\tau \sim p(\tau|\theta)} [R(\tau) | R(\tau) \geq \tilde{q}_\varepsilon(R)] \quad (5)$$

The gradient of the risk-seeking policy gradient can be estimated by:

$$\nabla_\theta J_{\text{risk}}(\theta; \varepsilon) \approx \frac{\lambda_{pg}}{\varepsilon N} \sum_{i=1}^N \left[ R(\tau^{(i)}) - \tilde{q}_\varepsilon(R) \right] \cdot \mathbf{1}_{R(\tau^{(i)}) \geq \tilde{q}_\varepsilon(R)} \nabla_\theta \log p(\tau^{(i)} | \theta) \quad (6)$$

where  $N$  denotes the total number of samples in a mini-batch; and  $\lambda_{pg}$  measures the importance of rewards. Note that  $\tilde{q}_\varepsilon$  is also chosen as the baseline reward and varies by the samples at each iteration. In addition, based on maximum entropy reinforcement-learning [29], the entropy value of each output action under the current policy is also required to be maximized to prevent generating a certain action continuously. The gradient of entropy can be expressed by:

$$\nabla_\theta J_{\text{entropy}}(\theta; \varepsilon) \approx \frac{1}{\varepsilon N} \sum_{i=1}^N \left( \lambda_{\mathcal{H}} \mathcal{H}(\tau^{(i)} | \theta) \right) \quad (7)$$

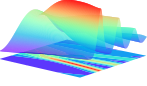
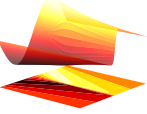
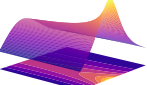
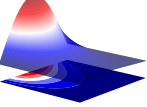
where  $\lambda_{\mathcal{H}}$  is the temperature parameter that controls the relative importance of the entropy term against the reward. By combining these two parts, the agent can be optimized to iteratively improve the best-case performance, while increasing the exploration ability to avoid getting stuck in local optima. The implementation details of the whole process are available on GitHub at <https://github.com/menggedu/DISCOVER>.

## 3 Results and discussions

### 3.1 Discovering open-form PDEs

We verified the accuracy and efficiency of our framework in mining open-form PDEs containing strong nonlinearities with little prior knowledge. Specifically, we reused the examples in SGA, including the Burgers' equation, the KdV equation, the Chafee-Infante equation, and PDE with compound terms (PDE\_compound) and fractional structure (PDE\_divide), to test the performance and compare it against SGA. The results show that our framework is not only accurate, but also computationally efficient and stable.

Table 1: Summary of discovered results for different PDEs of mathematical physics. The subscripts  $m$  and  $n$  denote the number of discretization.

	PDE discovered	Reward	Data discretization
	KdV $u_t = -0.5001(u * u)_x - 0.0025u_{xxx}$	$9.768 \times 10^{-1}$	$x \in [-1, 1]_{m=512}, t \in [0, 1]_{n=201}$
	Burgers $u_t = -1.0010uu_x + 0.1024u_{xx}$	$9.718 \times 10^{-1}$	$x \in [-8, 8]_{m=256}, t \in [0, 10]_{n=201}$
	Chafee-Infante $u_t = 1.0002u_{xx} - 1.0008u + 1.0004u^3$	$9.680 \times 10^{-1}$	$x \in [0, 3]_{m=301}, t \in [0, 0.5]_{n=200}$
	PDE_compound $u_t = 0.5002(u^2)_{xx}$	$9.874 \times 10^{-1}$	$x \in [1, 2]_{m=301}, t \in [0, 0.5]_{n=251}$
	PDE_divide $u_t = -0.9979u_x/x + 0.2498u_{xx}$	$9.413 \times 10^{-1}$	$x \in [1, 2]_{m=100}, t \in [0, 1]_{n=251}$

**Study case.** Five canonical models of mathematical physics: (1) **KdV equation:** It was jointly discovered by Dutch mathematicians Korteweg and De Vries to describe the one-way wave on shallow water [30]. It takes the form of  $u_t = auu_x + bu_{xxx}$ , where  $a$  is set to -1, and  $b$  is set to -0.0025. (2) **Burgers' equation:** As a nonlinear partial differential equation that simulates the propagation and reflection of shock waves, Burgers' equation is widely used in numerous fields, such as fluid mechanics, nonlinear acoustics, gas dynamics, etc.[31]. We consider a 1D viscous Burgers' equation  $u_t = -uu_x + vu_{xx}$ , where  $v$  is equal to 1 in this case. (3) **Chafee-Infante equation:** Another 1D nonlinear system is  $u_t = u_{xx} + a(u - u^3)$  with  $a = -1$ , which was developed by Nathaniel Chafee and Ettore Infante [32]. It has been broadly utilized in fluid mechanics, high-energy physical processes, electronics, and environmental research [33]. (4) **PDE\_compound and PDE\_divide:** These two equations are firstly put forward in SGA and used to demonstrate that our framework is capable of mining open-form PDEs, which is crucial for extracting unidentified and undiscovered governing equations from observations. PDE\_compound  $u_t = (uu_x)_x$  is proposed to describe viscous gravity current with compound function [34]. PDE\_divide  $u_t = -u_x/x + 0.25u_{xx}$  contains the fractional structure which conventional sparse regression methods cannot handle.

**Summary of discovered results.** The default hyperparameters used to mine the above PDEs are provided in Appendix B. Table 1 shows that under the premise of little prior knowledge, DISCOVER can mine the analytic representation of the various physical dynamics mentioned above, and the discovered equation form is accurate and concise (reward is basically close to 1). It is worth noting that the KdV equation, the Burgers' equation, and the Chafee-Infante equation can be discovered correctly by conventional sparse regression and genetic algorithms, but not for the PDE\_compound and PDE\_divide equations. This is mainly because these methods rely on a limited or conditional set of candidates, and cannot handle equations that contain compound terms or fractional structures. The result demonstrates that our proposed method can directly mine open-form equations from data, which offers wider application scenarios and practicability.

### 3.2 Comparisons to SGA

Since SGA can also uncover the equation representations of these five physical dynamics correctly, we will compare the specific performance (time consumption and accuracy) of DISCOVER based on RL and SGA based on GA. Note that all of the experiments were replicated with five different random seeds for each PDE. As shown in Table 2, the left column represents the MSE between the left-hand and right-hand side of the discovered equations. Both DISCOVER and SGA are capable of mining all terms of the equation exactly, but their coefficients of function terms are slightly different, resulting in the former having slightly smaller errors than the latter in the first four equations. The right column

Table 2: Comparison of MSE of discovered results and running time for DISCOVER and SGA. SGA (fast) is an optimized version of the original article code, with a faster computation speed. SGA(no  $u$ ) represents an accelerated version without prior knowledge  $u$ .

	MSE		Runing Time (s)			
	DISCOVER	SGA	DISCOVER	SGA	SGA(fast)	SGA(no $u$ )
KdV	$3.16 \times 10^{-5}$	$1.48 \times 10^{-4}$	<b>243.66</b>	1464.80	890.50	\
Burgers	$4.89 \times 10^{-7}$	$4.33 \times 10^{-5}$	<b>206.76</b>	495.18	423.8	\
Chafee-infante	$1.36 \times 10^{-4}$	$4.72 \times 10^{-4}$	67.23	27.70	<b>20.12</b>	>1000
PDE_compound	$8.31 \times 10^{-6}$	$4.56 \times 10^{-5}$	<b>13.31</b>	604.10	557.20	\
PDE_divide	$7.64 \times 10^{-4}$	$1.78 \times 10^{-4}$	<b>1259.53</b>	2046.24	1466.51	\

of Table 2 demonstrates the time consumed by the two methods to find the optimal equation. It can be seen that, in addition to the Chafee-Infante equation, our method uses only approximately 2% (PDE\_compound)-85% (PDE\_divide) of the time cost by SGA, which has higher computational efficiency. This is mainly because our method is model-based, and the entire optimization process is directional with a positive gain. As the iteration proceeds, the generated equations become increasingly reminiscent of the authentic expression. Additional details of the optimization process can be found in Appendix C. In contrast, SGA expands the diversity of the generated equation representations mainly through crossover and mutation of gene fragments, which is more stochastic and uncontrollable. Although it facilitates the search for more complex equations, it also leads to more training time.

It is worth noting that in the process of uncovering the Chafee-Infante equation, SGA takes  $u$  as a default function term (this information itself is known and easily accessible). By introducing this prior knowledge, the optimal form of the equation can always be easily found in the first round of iterations. Without this knowledge, however, SGA is unable to find the correct form of the equation within 300 iterations (>1000 s). The main reason for this problem is that SGA is modeled based on function terms, and each function term is represented by a multi-layer tree structure, while the term  $u$  is represented as a one-layer root node. It is difficult for SGA to obtain such a simple tree structure by crossover and mutation. DISCOVER models the equation as a whole and then partitions it according to the operators ("+" or "-"). Consequently, both simple and complex function terms can be handled easily. It can be seen that our method is time-efficient and has better practicality with little prior knowledge.

### 3.3 Comparison between structure-aware LSTM and standard LSTM

Our model introduces structured information in the agent, so that LSTM can attend to the previously generated tokens and equation structure when predicting the current output. However, the standard LSTM agent can only obtain the information from the last token and the composite history information coupled in the memory cell. To highlight the rationality and superiority of our model, we compare the performance of the two settings in the above four equations with other hyperparameters being the same. Since the PDE\_compound equation is relatively simple, no specific comparison is made here. Figure 3 (A-D) shows the distribution of the rewards under two agent settings during the training process. Since our model can better capture the structural and long-distance information in the equation, the expressions generated in each iteration are closer to the real one and then lead to larger rewards. Figure 3 (E) illustrates the number of iterations for discovering the optimal equation form. It can be seen that, except that the PDE\_divide equation is relatively close, the structure-aware LSTM can find the correct equation form with fewer iterations with almost no increase in the amount of computation.

## 4 Conclusions and future work

We propose a framework that can accurately explore open-form PDEs based on enhanced deep reinforcement-learning and symbolic representations. It can deal with compound terms and fractional structures that fixed candidate library based methods, such as SINDy, cannot handle. At the same time, our framework achieves more efficient and stable performance compared to GA-based methods (e.g., SGA). Moreover, the structure-aware architecture is capable of learning the PDE expressions more effectively compared with standard LSTM and can be applied to other problems with structured inputs. Our framework is also more scalable and practical, and can be applied to high-dimensional

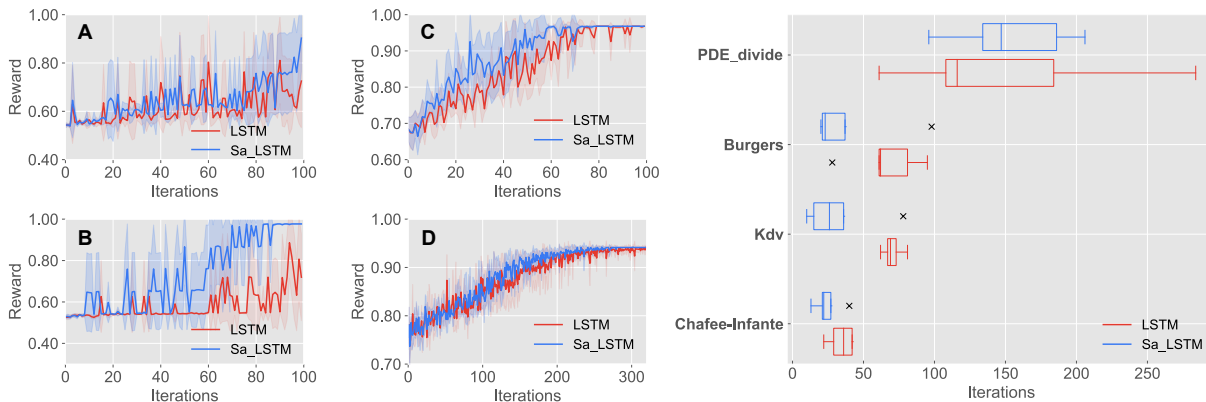


Figure 3: (A)-(D): Max reward distribution for four PDEs: (A): Burgers’ equation; (B):KdV equation; (C): Chafee-infante equation; (D): PDE\_divide. e. Iterations needed to discover the correct equation. Sa\_LSTM refers to the proposed sturcture-aware LSTM agent.

systems with multiple state variables, which will constitute our future work. In addition, we intend to further explore how DISCOVER performs on noisy observations.

## References

- [1] Steven L Brunton, Joshua L Proctor, and J Nathan Kutz. Discovering governing equations from data by sparse identification of nonlinear dynamical systems. *Proceedings of the national academy of sciences*, 113(15):3932–3937, 2016.
- [2] S. H. Rudy, S. L. Brunton, J. L. Proctor, and J. N. Kutz. Data-driven discovery of partial differential equations. 2016.
- [3] Daniel E Shea, Steven L Brunton, and J Nathan Kutz. Sindy-bvp: Sparse identification of nonlinear dynamics for boundary value problems. *Physical Review Research*, 3(2):023255, 2021.
- [4] Kadierdan Kaheman, J Nathan Kutz, and Steven L Brunton. Sindy-pi: a robust algorithm for parallel implicit sparse identification of nonlinear dynamics. *Proceedings of the Royal Society A*, 476(2242):20200279, 2020.
- [5] Daniel A Messenger and David M Bortz. Weak sindy for partial differential equations. *Journal of Computational Physics*, 443:110525, 2021.
- [6] Urban Fasel, J Nathan Kutz, Bingni W Brunton, and Steven L Brunton. Ensemble-sindy: Robust sparse model discovery in the low-data, high-noise limit, with active learning and control. *Proceedings of the Royal Society A*, 478(2260):20210904, 2022.
- [7] Zichao Long, Yiping Lu, Xianzhong Ma, and Bin Dong. Pde-net: Learning pdes from data. In *International Conference on Machine Learning*, pages 3208–3216. PMLR, 2018.
- [8] Zichao Long, Yiping Lu, and Bin Dong. Pde-net 2.0: Learning pdes from data with a numeric-symbolic hybrid deep network. *Journal of Computational Physics*, 399:108925, 2019.
- [9] Hao Xu, Haibin Chang, and Dongxiao Zhang. Dlga-pde: Discovery of pdes with incomplete candidate library via combination of deep learning and genetic algorithm. *Journal of Computational Physics*, 418:109584, 2020.
- [10] Yuntian Chen, Yingtao Luo, Qiang Liu, Hao Xu, and Dongxiao Zhang. Symbolic genetic algorithm for discovering open-form partial differential equations (sga-pde). *Physical Review Research*, 4(2):023174, 2022.
- [11] Michael Schmidt and Hod Lipson. Distilling free-form natural laws from experimental data. *science*, 324(5923):81–85, 2009.
- [12] Josh Bongard and Hod Lipson. Automated reverse engineering of nonlinear dynamical systems. *Proceedings of the National Academy of Sciences*, 104(24):9943–9948, 2007.
- [13] Douglas Adriano Augusto and Helio JC Barbosa. Symbolic regression via genetic programming. In *Proceedings. Vol. 1. Sixth Brazilian Symposium on Neural Networks*, pages 173–178. IEEE, 2000.
- [14] Sheng Sun, Runhai Ouyang, Bochao Zhang, and Tong-Yi Zhang. Data-driven discovery of formulas by symbolic regression. *MRS Bulletin*, 44(7):559–564, 2019.

- [15] Samaneh Sadat Mousavi Astarabadi and Mohammad Mehdi Ebadzadeh. Genetic programming performance prediction and its application for symbolic regression problems. *Information Sciences*, 502:418–433, 2019.
- [16] Maryam Amir Haeri, Mohammad Mehdi Ebadzadeh, and Gianluigi Folino. Statistical genetic programming for symbolic regression. *Applied Soft Computing*, 60:447–469, 2017.
- [17] Georg Martius and Christoph H Lampert. Extrapolation and learning equations. *arXiv preprint arXiv:1610.02995*, 2016.
- [18] Subham Sahoo, Christoph Lampert, and Georg Martius. Learning equations for extrapolation and control. In *International Conference on Machine Learning*, pages 4442–4450. PMLR, 2018.
- [19] Fangzheng Sun, Yang Liu, Jian-Xun Wang, and Hao Sun. Symbolic physics learner: Discovering governing equations via monte carlo tree search. *arXiv preprint arXiv:2205.13134*, 2022.
- [20] Brenden K Petersen, Mikel Landajuela Larma, Terrell N Mundhenk, Claudio Prata Santiago, Soo Kyung Kim, and Joanne Taery Kim. Deep symbolic regression: Recovering mathematical expressions from data via risk-seeking policy gradients. In *International Conference on Learning Representations*, 2020.
- [21] Hengzhe Zhang and Aimin Zhou. Rl-gep: Symbolic regression via gene expression programming and reinforcement learning. In *2021 International Joint Conference on Neural Networks (IJCNN)*, pages 1–8. IEEE, 2021.
- [22] T Nathan Mundhenk, Mikel Landajuela, Ruben Glatt, Claudio P Santiago, Daniel M Faissol, and Brenden K Petersen. Symbolic regression via neural-guided genetic programming population seeding. *arXiv preprint arXiv:2111.00053*, 2021.
- [23] Silviu-Marian Udrescu and Max Tegmark. Ai feynman: A physics-inspired method for symbolic regression. *Science Advances*, 6(16):eaay2631, 2020.
- [24] Lynne Billard and Edwin Diday. Symbolic regression analysis. In *Classification, clustering, and data analysis*, pages 281–288. Springer, 2002.
- [25] Thomas Elsken, Jan Hendrik Metzen, and Frank Hutter. Neural architecture search: A survey. *The Journal of Machine Learning Research*, 20(1):1997–2017, 2019.
- [26] Aviv Tamar, Yonatan Glassner, and Shie Mannor. Policy gradients beyond expectations: Conditional value-at-risk. *arXiv preprint arXiv:1404.3862*, 2014.
- [27] Aviv Tamar, Yonatan Glassner, and Shie Mannor. Optimizing the cvar via sampling. In *Twenty-Ninth AAAI Conference on Artificial Intelligence*, 2015.
- [28] Takuya Hiraoka, Takahisa Imagawa, Tatsuya Mori, Takashi Onishi, and Yoshimasa Tsuruoka. Learning robust options by conditional value at risk optimization. *Advances in Neural Information Processing Systems*, 32, 2019.
- [29] Tuomas Haarnoja, Aurick Zhou, Pieter Abbeel, and Sergey Levine. Soft actor-critic: Off-policy maximum entropy deep reinforcement learning with a stochastic actor. In *International conference on machine learning*, pages 1861–1870. PMLR, 2018.
- [30] DJ Kordeweg and G de Vries. On the change of form of long waves advancing in a rectangular channel, and a new type of long stationary wave. *Philos. Mag.*, 39:422–443, 1895.
- [31] Johannes Martinus Burgers. A mathematical model illustrating the theory of turbulence. *Advances in applied mechanics*, 1:171–199, 1948.
- [32] Alan C. Newell and J. A. Whitehead. Finite bandwidth, finite amplitude convection. *Journal of Fluid Mechanics*, 38(2):279–303, 1969.
- [33] Alper Korkmaz. Complex wave solutions to mathematical biology models i: Newell–whitehead–segel and zeldovich equations. *Journal of Computational and Nonlinear Dynamics*, 13(8):081004, 2018.
- [34] GHF Gardner, J Downie, and HA Kendall. Gravity segregation of miscible fluids in linear models. *Society of Petroleum Engineers Journal*, 2(02):95–104, 1962.
- [35] Kyunghyun Cho, Bart Van Merriënboer, Caglar Gulcehre, Dzmitry Bahdanau, Fethi Bougares, Holger Schwenk, and Yoshua Bengio. Learning phrase representations using rnn encoder-decoder for statistical machine translation. *arXiv preprint arXiv:1406.1078*, 2014.
- [36] Lifen Li and Tianyu Zhang. Research on text generation based on lstm. *International Core Journal of Engineering*, 7(5):525–535, 2021.
- [37] Yequan Wang, Minlie Huang, Xiaoyan Zhu, and Li Zhao. Attention-based lstm for aspect-level sentiment classification. In *Proceedings of the 2016 conference on empirical methods in natural language processing*, pages 606–615, 2016.

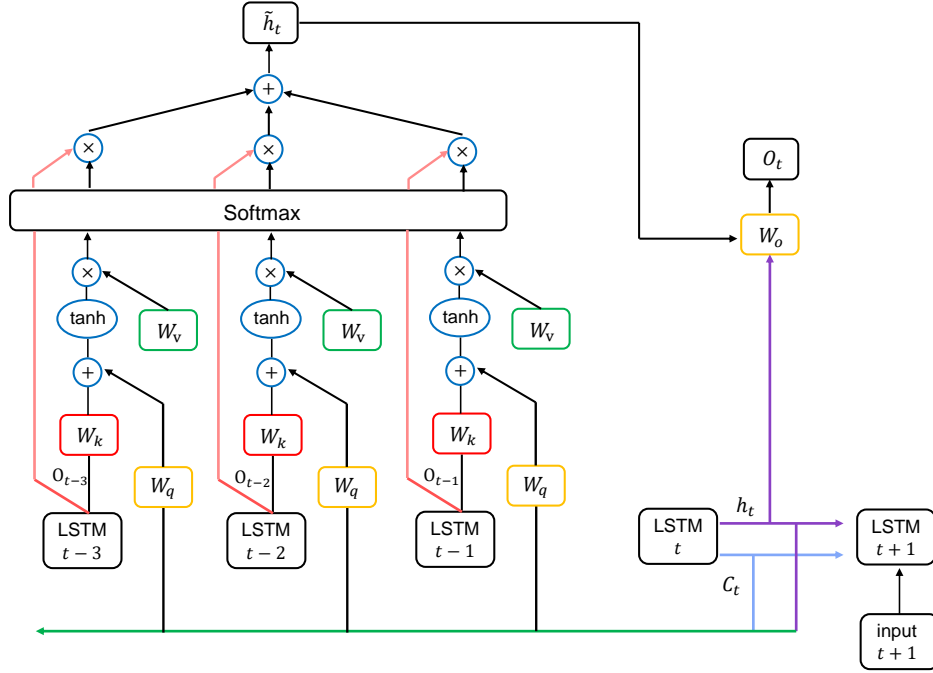


Figure A1: The architecture of monotonic attention. Only the information of the past three time-steps is integrated here. In fact, the time span can be set longer, so that it can focus on further historical information.

- [38] Youru Li, Zhenfeng Zhu, Deqiang Kong, Hua Han, and Yao Zhao. Ea-lstm: Evolutionary attention-based lstm for time series prediction. *Knowledge-Based Systems*, 181:104785, 2019.
- [39] Jianpeng Cheng, Li Dong, and Mirella Lapata. Long short-term memory-networks for machine reading. *arXiv preprint arXiv:1601.06733*, 2016.
- [40] Martín Abadi, Paul Barham, Jianmin Chen, Zhifeng Chen, Andy Davis, Jeffrey Dean, Matthieu Devin, Sanjay Ghemawat, Geoffrey Irving, Michael Isard, et al. {TensorFlow}: a system for {Large-Scale} machine learning. In *12th USENIX symposium on operating systems design and implementation (OSDI 16)*, pages 265–283, 2016.

## Appendix A Monotonic attention

It is well known that the LSTM recurrent neural network is effective at dealing with sequence problems, such as machine translation [35] and text generation [36]. The history information is recursive-compressed and stored in a memory cell, and three gates, including an input gate, an output gate, and a forget gate, control the flow of the information and decision-making. However, its constraint is obvious, i.e., prediction of the current time-step largely depends on the adjacent units, and recursively updating the information destroys the structural information of the input. Furthermore, the storage capacity of memory cells is limited, and information loss increases as the sequence grows. Some attempts have been made to incorporate soft attention to reason over structure and directly select useful information from the previous tokens [37, 38, 39].

In order to capture the long-distance dependencies and structural information, we wrapped the original LSTM with a monotonic attention layer (MAL), which mainly draws on the architecture and configuration in LSTMN [39]. Attention memory is utilized here to simulate the human brain to read historical information and mine the relationship between them. The architecture of MAL is illustrated in Figure A1. Compared with the standard LSTM, an extra hidden vector  $\tilde{h}_t$  is introduced to store the relations between tokens. At time-step  $t$ , an attention function can be calculated by:

$$[h_t, c_t] = \text{LSTM}(x_t, [h_{t-1}, c_{t-1}]) \quad (\text{A1})$$

$$a_i^t = W_v^T \tanh(W_q [h_t, c_t] + W_k O_i) \quad (\text{A2})$$

$$s_i^t = \text{softmax}(a_i^t) \tag{A3}$$

where  $W_q$ ,  $W_k$ , and  $W_v$  are the parameter matrices used to linearly project queries, keys, and their output, respectively. The state vector  $s_t$  denotes a probability distribution over the previous inputs to measure the degree of attention to historical information. It is also used to calculate our new hidden vector. By combining  $\tilde{h}_t$  containing the relation information and the original hidden vector  $h_t$ , the final output can be represented as follows:

$$\tilde{h}_t = \sum_i^{t-1} s_i^t O_i \tag{A4}$$

$$O_t = W_o [h_t, \tilde{h}_t] \tag{A5}$$

The specific implementation refers to the source code in TensorFlow [40], and some modifications are made to better combine structured input.

## Appendix B Hyperparameters

The default hyperparameters used to mine the above PDEs are shown in Table B1. As mentioned above, we use the plus or minus operator that appears at the top level of the tree as the identifiers to split the equation into several function terms. We require that the number of their occurrences should not exceed five, which means that the generated expressions can only be spliced into at most six function terms. The parsimony penalty factor which guarantees the simplicity of the equation is set to 0.01. In each iteration, the agent will generate a total of  $N = 500$  PDE expressions. Finally, after filtering the illegal expressions and low rewards, only 2% ( $\varepsilon = 0.02$ ) of the total expressions, i.e., 10 equations with the highest reward, are selected for the update of the agent. In the optimization process, the coefficients of entropy loss and policy gradient loss are set to 0.03 and 1, respectively.

Table B1: Default hyperparameter settings for discovering open-form PDEs.

Hyperparameter	Default value	Definition
$N_{subtree}$	6	Number of function terms
$\zeta$	0.01	Parsimony penalty factor
$N$	500	Total generated expressions at each iteration
$\varepsilon$	0.02	Threshold of reserved expressions
$\lambda$	0	Weight of the STRidge regularization term
$tol$	$1 \times 10^{-4}$	Threshold of reserved function terms
$\lambda_{\mathcal{H}}$	0.03	Coefficients of entropy loss
$\lambda_{pg}$	1	Coefficients of policy gradient loss

## Appendix C The optimization process of DISCOVER

To demonstrate the concrete details of the optimization process, we take PDE\_divide as an example to show the reward distribution and evolution of the discovered equation. Figure C1 below shows the reward distribution of the best-performing, top  $\varepsilon$ , and the mean of the top  $\varepsilon$  in each batch during the training process. It can be seen that as the iteration progresses, the maximum reward is gradually increased and gets closer to 1 at the end. Figure C2 clearly illustrates the evolution process of the generated equation expressions during the iteration process. It can be seen that from the 1st to the 99th iteration, the composition of the equation terms gradually approaches the correct one. The increase in reward gradually benefits from the increase in accuracy. From the 99th iteration to the 136th iteration, in addition to a further gain of accuracy, the parsimony of the expressions is also considered. Therefore, in the process of revealing equations from the data, when the accuracy of the generated terms is similar, the expressions with fewer terms have a bigger reward. This also ensures that the final equation form is both accurate and parsimonious.

## Appendix D Ablation study

Based on the theory of risk-seeking policy gradient, only  $\varepsilon$  fraction of the best expressions is selected to update the agent during the training process to improve the best-case performance. The learning effect and calculation time are directly



impacted by the quality and number of the expressions at each iteration. It is mainly affected by two hyperparameters: the total number of generated expressions at each iteration  $N$ , and the quantile of the rewards  $\varepsilon$  used to filter expressions. Then, we focus on discussing their specific impact on the entire optimization process.

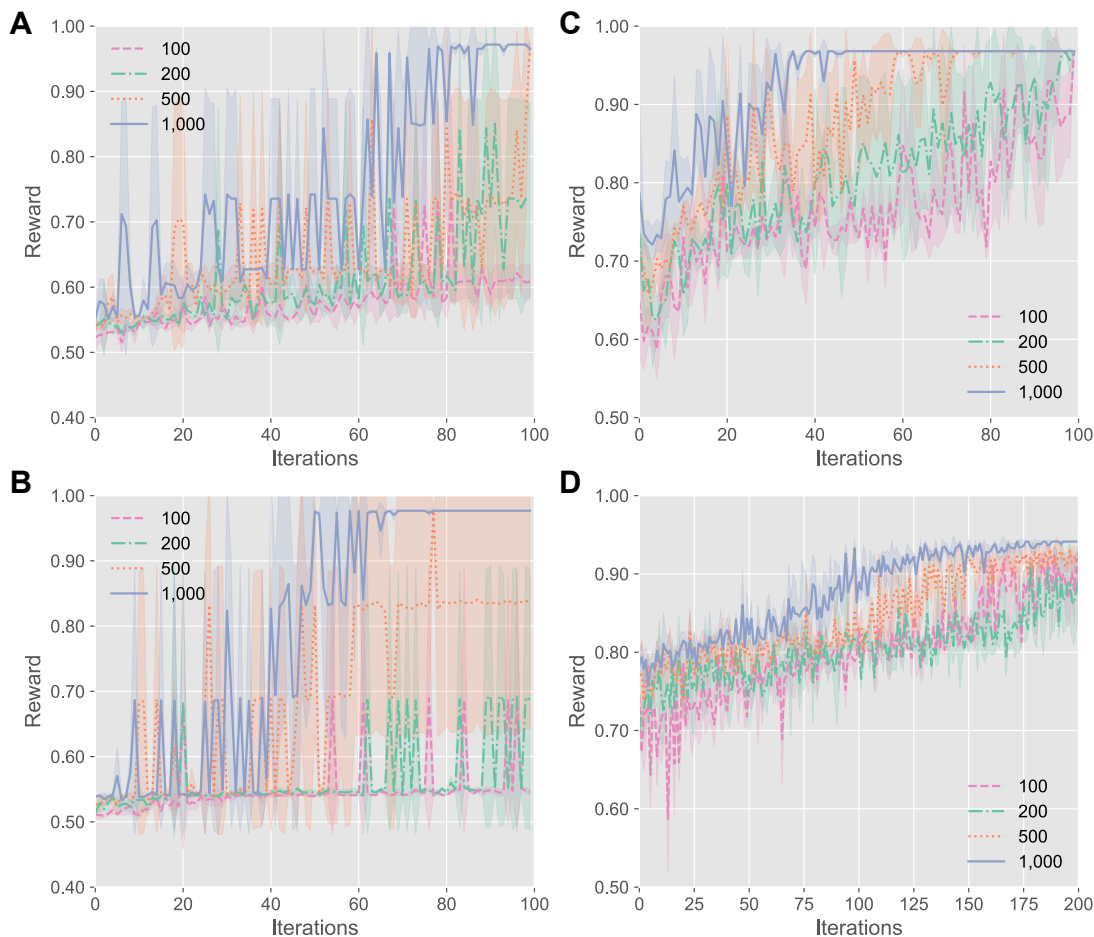


Figure D1: (A)-(D): Maximum reward distribution with different  $N$  for four PDEs: (A): Burgers' equation; (B): KdV equation; (C): Chafee-Infante equation; (D): PDE\_divide.

Figure D1 illustrates the maximum reward distribution of four different PDEs with different  $N$ . It is obvious that the more expressions are produced in each round, the better the expressions that are ultimately chosen to update the agent, and the fewer iterations it takes to find the optimal equation. However, it is worth noting that generating more expressions also takes more computation resources, and a trade-off needs to be found between the number of generated expressions and the time consumed. In the actual training process, it is necessary to generate as many expressions as possible, especially at the beginning, to avoid getting stuck in local optima. The other parameter  $\varepsilon$  determine the proportion of the expressions generated in each round that can actually be used to update the agent. When the parameter is set to 0, all expressions will be used for the update of the agent, which is the standard policy gradient approach. As shown in Figure D2, choosing a relatively small and reasonable parameter is necessary for the agent to learn the optimal solution, which can speed-up the training process. However, with the method of policy gradient, each time it is expected that the rewards of all expressions in each batch are maximized, which obviously slows down the update speed, and may even fail to find the final correct expression.

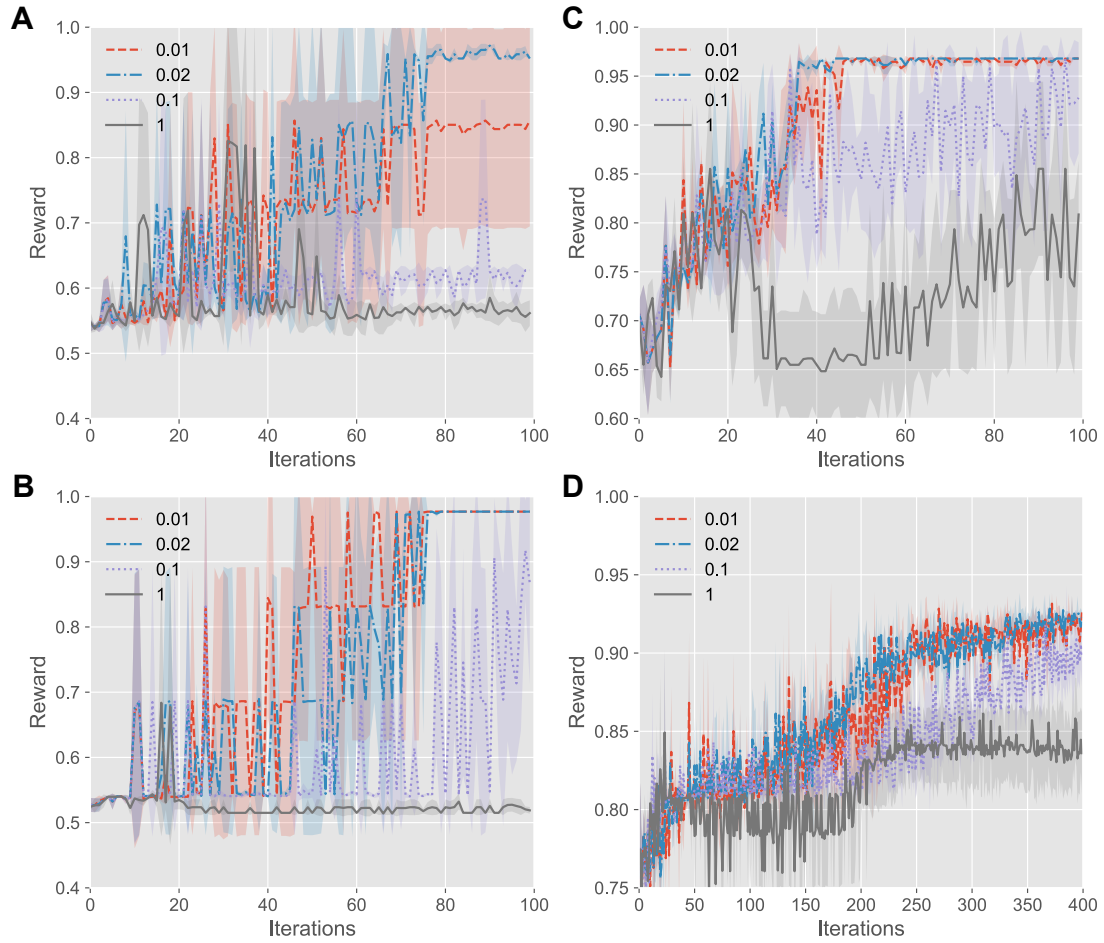


Figure D2: (A)-(D): Maximum reward distribution with different  $\epsilon$  for four PDEs: (A): Burgers' equation; (B):KdV equation; (C): Chafee-Infante equation; (D): PDE\_divide.